

Determination of local effects for chloroaluminate ionic liquids on Diels–Alder reactions

Orlando Acevedo *

Department of Chemistry and Biochemistry, Auburn University, Auburn, AL 36849, United States

ARTICLE INFO

Article history:

Received 16 December 2008

Received in revised form 31 March 2009

Accepted 11 April 2009

Available online 19 April 2009

Keywords:

Ionic liquids

Diels–Alder reaction

Density functional theory (DFT)

Chloroaluminates

Catalysis

ABSTRACT

Room temperature ionic liquids are an exciting class of solvents that have the potential to accelerate and control a vast range of reactions. The Diels–Alder reaction, paradigm in organic synthesis, highlights the advantages provided by ionic liquids as the reaction between cyclopentadiene and methyl acrylate in 1-ethyl-3-methylimidazolium tetrachloroaluminate and heptachlorodialuminate [EMIM][AlCl₄] and [EMIM][Al₂Cl₇], respectively, has been reported to react with rates over 200 times faster and *endo* selectivity 10 times greater than commonly used reaction conditions. Density functional theory (DFT) calculations at the B3LYP/6-311+G(2d,p) theory level have been employed to determine the origin of the reported rate accelerations. The DFT simulations find that specific hydrogen bonding between the ionic liquid cations and the dienophile at the transition state is primarily responsible, however, the rate of reaction was found to be moderated by the solvent's hydrogen bond accepting ability (anion effect). Different anion-to-cation ratios were tested and a 1:1 ratio was determined to give the best agreement with experimental observations. The computed DFT activation barriers were within reasonable agreement of the reported rates, however it is clear that a full microenvironment featuring hundreds of ions is necessary for proper computational treatment of the solvent effects delivered by the ionic liquids.

© 2009 Elsevier Inc. All rights reserved.

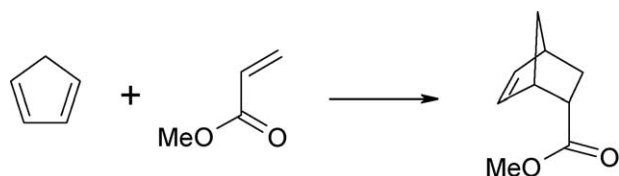
1. Introduction

The use of ionic liquids as a reaction medium for chemical reactions has dramatically increased in recent years, due in large part to numerous reported advances in catalysis [1], separation science [2], and organic synthesis [3] when employing the unique solvents. However, only a few systematic studies have addressed the microscopic details on how ionic liquids influence chemical reactivity and selectivity [4–7]. Of specific interest are the large rate accelerations and stereoselectivity enhancements reported for the Diels–Alder reaction between cyclopentadiene and methyl acrylate (Scheme 1) in chloroaluminate ionic liquids, particularly when compared to common organic solvents or water [8,9]. The mechanism behind the ionic liquid's impact on the reaction is not well understood, although recent studies featuring the “basic” and “acidic” ionic liquid melts 1-ethyl-3-methylimidazolium tetrachloroaluminate [EMIM][AlCl₄] and 1-ethyl-3-methylimidazolium heptachlorodialuminate [EMIM][Al₂Cl₇], respectively, have suggested that hydrogen bonding is primarily responsible [5,6]. High internal solvent pressure [10], solvent polarity [11] and Lewis acidity [12] may also contribute to the phenomena.

Our recent mixed quantum and molecular mechanical (QM/MM) investigation of the Diels–Alder reaction between cyclopentadiene and methyl acrylate featured the PDDG/PM3 semi-empirical molecular orbital method [13] to treat the reacting system, while custom OPLS-AA parameters were used to simulate hundreds of ions in the liquid environment [5]. The reported calculations overestimated the experimental activation barriers, but the relative rates of reaction were well reproduced between the chloroaluminate ionic liquids [EMIM][AlCl₄] and [EMIM][Al₂Cl₇], as well as water and 1-chlorobutane [5]. The use of density functional theory (DFT) methodology on a small number of explicit cation and anion combinations complexed to the reacting substrates may help elucidate the local interactions responsible for the observed rate acceleration while providing improved thermodynamic agreement with experiment. Representation of solvation effects by discrete models incorporating a few key molecules at specific interacting sites has been successful for other Diels–Alder reactions [14–16]. As such, B3LYP/6-311+G(2d,p) calculations have been carried out to systematically investigate the effect of the [EMIM] cation upon the Diels–Alder transition structure and the consequences of [AlCl₄] and [Al₂Cl₇] anion participation in the reaction. Gas-phase ion pairs between [EMIM] and the chloroaluminates, including [Al₃Cl₁₀], were computed in anion-to-cation ratios of 1:1 and 2:1. Reactants and transition structures for the Diels–Alder reaction between

* Tel.: +1 334 844 6549; fax: +1 334 844 6959.

E-mail address: orlando.acevedo@auburn.edu.



Scheme 1. Diels–Alder reaction between cyclopentadiene and methyl acrylate.

cyclopentadiene and methyl acrylate were subsequently complexed with ion ratios of 0:1, 1:1, and 2:1 to elucidate local effects from the ionic liquids on the system and to gauge any possible cation modulation via the anions.

2. Computational methods

Density functional theory calculations at the B3LYP theory level [17] with the 6-31G(d) and 6-311+G(2d,p) basis sets were used to characterize the ionic liquid ground states and Diels–Alder transition structures using the program Gaussian 03 [18]. DFT has been shown to produce realistic structures and energies for the components of ionic liquids [6]. Electron correlation is significant in describing the electronics of ionic liquids, which has been successfully applied to molten salts [19]. Earlier findings have shown that larger basis sets, such as 6-311G(3df), with the B3LYP

method do not change the energetics or structures of chloroaluminate containing systems, as compared to the smaller 6-31G(d) basis set [20]. MP2 calculations have also been used to validate B3LYP as an appropriate level of theory for the ion pairs, since both methods give similar energetic and geometrical results. B3LYP/6-31G(d) and B3LYP/6-311+G(2d,p) methods were used for energy optimizations and vibrational frequency calculations, which confirmed all stationary points as either minima or transition structures, provided thermodynamic and zero-point energy corrections, and reproduced the vibrational spectrum. All calculations were performed on computers located at the Alabama Supercomputer Center.

3. Results and discussion

3.1. Ionic liquid models

An attractive property exclusive to chloroaluminate-based ionic liquids is the ability to tune the Lewis acidity of the system through the composition of the liquid [21]. Raman [22], ^{27}Al NMR [23] and mass spectra [24] all indicate that when AlCl_3 comprises <50 mol% of the [EMIM][Cl] ionic liquid melt, $[\text{AlCl}_4]$ is the only chloroaluminate species present. These “basic” melts are composed of [EMIM], $[\text{AlCl}_4]$, and chloride ions that are not bound to aluminum. A ratio >1:1 AlCl_3 -to-[EMIM][Cl] is referred to as an

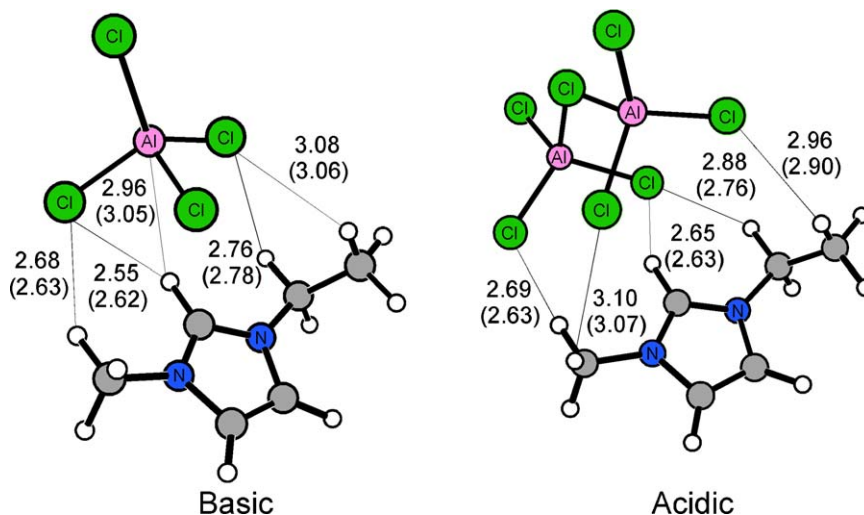


Fig. 1. B3LYP/6-31G(d) (MP2/6-31G(d) in parentheses) optimized structures of 1:1 ionic liquid complexes. Distances are in Å.

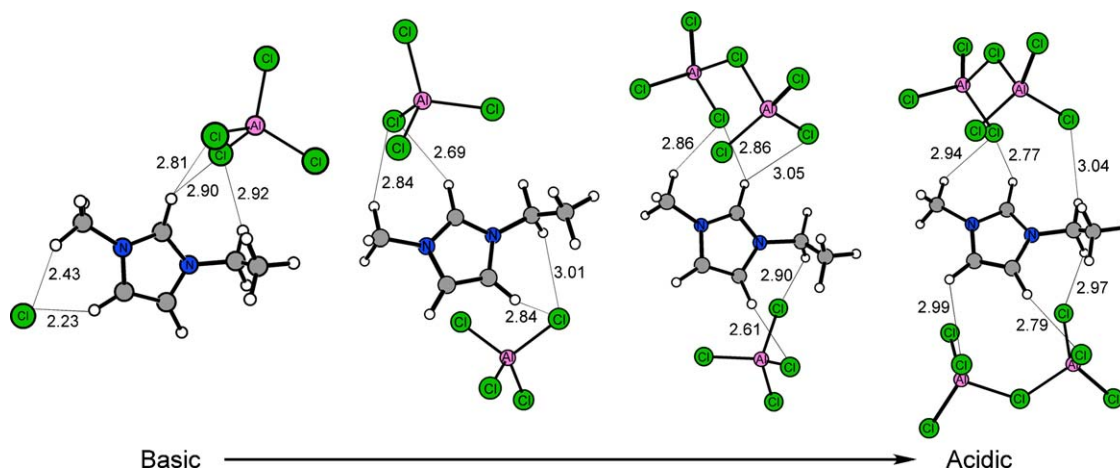


Fig. 2. B3LYP/6-31G(d) optimized structures of 2:1 ionic liquid complexes. Distances in Å.

“acidic” melt; ^{27}Al NMR [25] and negative-ion FAB mass spectra [26] have shown that $[\text{AlCl}_4]$ and $[\text{Al}_2\text{Cl}_7]$ are the principal anionic constituents in this case. When an “acidic” melt (51% AlCl_3) of $[\text{EMIM}][\text{Cl}]$ was used as the solvent for the Diels–Alder reaction in Scheme 1, the rate of reaction was 10, 175, and 560 times faster than in water, ethyl ammonium nitrate, and 1-chlorobutane, respectively [8]. However, the “basic” melt (48% AlCl_3) gave a rate 2.4 times slower than that of water.

To elucidate the role of the ions upon the reactivity of the Diels–Alder reaction, DFT and ab initio methods were initially employed to investigate the isolated ions which form in the “acidic” and “basic” melts, i.e. $[\text{AlCl}_4]$, $[\text{Al}_2\text{Cl}_7]$ and $[\text{EMIM}]$. An X-ray crystal structure of the “basic” melt involving $[\text{EMIM}][\text{Cl}]$ and AlCl_3 has been reported [27] and comparison of the B3LYP/6-31G(d) computed $[\text{EMIM}]$ cation geometry to the X-ray structure gave good agreement [6]. DFT calculations on $[\text{AlCl}_4]$ confirmed the anion to be tetrahedral in accordance with X-ray crystallographic results [28] and the geometry of $[\text{Al}_2\text{Cl}_7]$ has been found to be C_2 symmetric as verified through an IR spectrum [29].

In order to explore the differences between the “basic” and “acidic” melts, 1:1 and 2:1 ratios of anions-to-cations have been considered (Figs. 1 and 2). Nuclear magnetic resonance experiments on mixtures of $[\text{EMIM}][\text{Cl}]$ and AlCl_3 have shown that chemical shifts of protons in the cations are highly dependent on the ion proportion of the melt [30], and that the melts are relatively organized in the liquid state [30–32]. Intriguingly, the study discovered a systematic deviation when using a 1:1 pair model, while two anions per cation gave better agreement with experimental data [30].

Binding enthalpies for the 1:1 complexes were computed by subtracting the energy of the complex from energies for the separated ions. It was found that the HF, B3LYP, and MP2 theory levels all gave a similar trend (Table 1). As expected, the enthalpies decrease significantly as the chloroaluminate ion becomes larger and more delocalized. Fig. 1 shows the most acidic hydrogen in the 2-position of $[\text{EMIM}]$ at a distance of 2.55 Å to the nearest chlorine atom for the “basic” melt, while the “acidic” melt increases the interaction distance to 2.65 Å. The reduced ion-pairing in the “acidic” melt may allow for stronger intermolecular interactions to occur at the transition structure consistent with the proposed origin of the *endo*-selectivity for the Diels–Alder reaction [7]. Table 1 also includes an anionic species $[\text{Al}_3\text{Cl}_{10}]$ observed in “super-acidic” melts using mass and infrared spectrometry [33]. The computed binding enthalpy continued to decrease with the larger $[\text{Al}_3\text{Cl}_{10}]$ anion, confirming a weakening interaction with increased acidity.

For the 2:1 complexes, four alternatives with one $[\text{EMIM}]$ cation complexed to varying combinations of $[\text{Cl}]$, $[\text{AlCl}_4]$, and $[\text{Al}_2\text{Cl}_7]$

Table 1

Binding enthalpies, $-\Delta H$ (in kcal/mol), at 25 °C for 1:1 anion-to-cation ionic liquid models^a.

	HF	B3LYP	MP2
$[\text{EMIM}][\text{AlCl}_4]$	68.0 ^b	69.9	73.9
$[\text{EMIM}][\text{Al}_2\text{Cl}_7]$	63.2 ^b	63.9	68.5
$[\text{EMIM}][\text{Al}_3\text{Cl}_{10}]$	57.7	60.5	67.2

^a Optimized using the 6-31G(d) basis set.

^b Ref. [42].

Table 2

Binding enthalpies (kcal/mol) at 25 °C for the 2:1 anion-to-cation ionic liquid models^a.

	$-\Delta H$
$[\text{Cl}]\cdots[\text{EMIM}]\cdots[\text{AlCl}_4]$	111.0
$[\text{AlCl}_4]\cdots[\text{EMIM}]\cdots[\text{AlCl}_4]$	90.3
$[\text{Al}_2\text{Cl}_7]\cdots[\text{EMIM}]\cdots[\text{AlCl}_4]$	86.5
$[\text{Al}_2\text{Cl}_7]\cdots[\text{EMIM}]\cdots[\text{Al}_2\text{Cl}_7]$	83.6

^a Optimized using B3LYP/6-31G(d).

anions were considered (Fig. 2). When an $[\text{Al}_2\text{Cl}_7]$ anion is present, the melt is considered to be “acidic”, since the species is only found at >1:1 AlCl_3 -to- $[\text{EMIM}][\text{Cl}]$ ratios. Binding enthalpies are much larger for the 2:1 “acidic” and “basic” melts compared to the 1:1 complexes (Tables 1 and 2). However, the trend of reduced affinity as the chloroaluminate ion becomes larger is retained. The distance between the most acidic hydrogen on the $[\text{EMIM}]$ cation and the nearest chlorine in the complex with two $[\text{AlCl}_4]$ ions is 2.69 Å, and it increases to 2.77 Å with two $[\text{Al}_2\text{Cl}_7]$ ions.

Infrared studies of $[\text{EMIM}][\text{Cl}]$ ionic liquids have been carried out by Osteryoung [34]; allowing comparisons for specific vibrational stretches and bends with the present DFT frequency analysis on the 1:1, and 2:1 “acidic” and “basic” melt models (Table 3). The computed vibrational frequencies have been scaled by 0.9614 in all cases, which is appropriate for B3LYP/6-31G(d) [35]. The results for the 1:1 “acidic” and “basic” complexes are within 1.9 and 2.6% of the experimental values, respectively, while those for the 2:1 complexes agree within 1.8 and 2.3%. Previous investigations using the semi-empirical methods AM1 and MNDO gave large errors [29,32].

4. Transition structures

4.1. Parent system

The reaction between cyclopentadiene and methyl acrylate was first examined in vacuum using B3LYP/6-311+G(2d,p); the

Table 3

Comparison of peak frequency (cm^{-1}) changes with B3LYP/6-31G(d) at different melt ratios.

Melt	Aromatic C–H str.	Aliphatic C–H str.	$-\text{C}\equiv\text{N}$ -str.	Ring str.	Ring i/p b	Ring o/p b
$[\text{EMIM}]^a$	3183	3039	1550	1139	794	717
Acidic						
$[\text{EMIM}][\text{Al}_2\text{Cl}_7]^b$	3176	2970	1547	1140	837	710
$[\text{EMIM}][\text{Al}_2\text{Cl}_7][\text{AlCl}_4]^c$	3161	2979	1552	1146	808	726
$[\text{EMIM}]-2[\text{Al}_2\text{Cl}_7]^c$	3180	2982	1552	1148	810	730
1.50:1 melt ^d	3161	2992	1595	1169	836	747
Basic						
$[\text{EMIM}][\text{AlCl}_4]^b$	3152	2971	1549	1140	867	712
$[\text{EMIM}]-[\text{AlCl}_4]-[\text{Cl}]^c$	3181	2943	1558	1151	793	715
$[\text{EMIM}]-2[\text{AlCl}_4]^c$	3168	2969	1553	1147	841	725
0.55:1 melt ^d	3154	2983	1590	1175	838	758

All calculations scaled by 0.9614.

^a 0:1 ratio.

^b 1:1 ratio.

^c 2:1 ratio.

^d Experimental data taken from Ref. [34].

Table 4

Activation thermodynamics (kcal/mol) for the *endo-cis* transition structure between cyclopentadiene and methyl acrylate in gas and with 1:1 and 2:1 ionic liquid models using B3LYP/6-31G(d).

TS	ΔE^\ddagger_0	ΔE^\ddagger_{298}	ΔH^\ddagger_{298}	ΔG^\ddagger_{298}
Gas	17.7	17.5	16.9	30.6
Basic				
[EMIM][AlCl ₄]	9.0	10.3	9.1	32.4
[EMIM] + 2[AlCl ₄]	11.4	12.7	11.5	35.8
Acidic				
[EMIM][Al ₂ Cl ₇]	8.1	9.3	8.1	31.9
[EMIM] + [Al ₂ Cl ₇] + [AlCl ₄]	11.7	12.9	11.8	35.8
[EMIM] + 2[Al ₂ Cl ₇]	12.1	13.2	12.0	38.4

Table 5

Activation thermodynamics (kcal/mol) for the *endo-cis* transition structure between cyclopentadiene and methyl acrylate in gas and with 1:1 anion-to-cation ionic liquid models using B3LYP/6-311+G(2d,p).

TS	ΔE^\ddagger_0	ΔE^\ddagger_{298}	ΔH^\ddagger_{298}	ΔG^\ddagger_{298}
Gas	21.6	21.4	20.8	34.6
[EMIM][AlCl ₄]	14.1	15.7	14.5	37.5
[EMIM][Al ₂ Cl ₇]	13.7	14.9	13.8	37.6

predicted activation enthalpy was 20.8 kcal/mol at 25 °C for the *endo-cis* transition structure ($\Delta H^\ddagger = 16.9$ kcal/mol at the B3LYP/6-31G(d) theory level, see Tables 4 and 5). The experimental activation enthalpy is 15.1 kcal/mol, when determined in toluene [36]. To address the difference in media, it is noted that the activation enthalpy for a similar Diels–Alder reaction between acrolein and butadiene was computed to drop by approximately 1.5 kcal/mol in going from vacuum to benzene (similar dielectric to toluene) [15]. Consequently, increasing the solution-phase experimental value by 1.5 kcal/mol would give a gas phase activation barrier of 16.6 kcal/mol, which is reasonably consistent with the computed values for the reaction with methyl acrylate.

4.2. Complexation of an [EMIM] cation

The Diels–Alder reaction in the presence of a single [EMIM] cation was then considered. The *endo-cis*, *endo-trans*, *exo-cis*, and *exo-trans* transition structures were located for the reaction using four different configurations with the [EMIM] cation. The most acidic imidazolium proton (on C2, $pK_a = 21$ –23) [37] was oriented towards the carbonyl oxygen of methyl acrylate in conformations **2** and **3**, while interaction with the ring hydrogens on C4 and C5 was considered in **1** and **4**. Stronger complexation with the carbonyl

oxygen was found for **2** and **3** with O–H distances of 1.95–1.96 Å compared to distances on **1** and **4** of 2.04–2.06 Å (*endo-cis*; Fig. 3). In addition, the carbonyl oxygen appeared to form weaker electrostatic interactions with a hydrogen in the cation's methyl (**1** and **2**) or ethyl (**3** and **4**) group. The transition structures were asynchronous, as indicated by the lengths of the breaking and forming bonds (~ 2.03 and ~ 2.56 Å). Structures **2** and **3** also gave more favorable interaction enthalpies by roughly 2 kcal/mol (see Supporting Information Table S1). Transition structure **2** has the lowest-energy and the relative activation enthalpies of **1**, **3**, and **4** are 2.9, 1.2, and 2.3 kcal/mol, respectively. The present results are consistent with the general view that rate accelerations for Diels–Alder reactions in protic solvents arise from enhanced hydrogen-bonding to hydrogen-bond accepting groups in the dienophile [38]. However, the model is an oversimplification of the environment found in an ionic liquid considering that no anions were present.

4.3. 1:1 “acidic” and “basic” melts

With the most favorable orientation of the [EMIM] cation located, the [AlCl₄] and [Al₂Cl₇] anions were added and the transition structure complexes were re-optimized using B3LYP

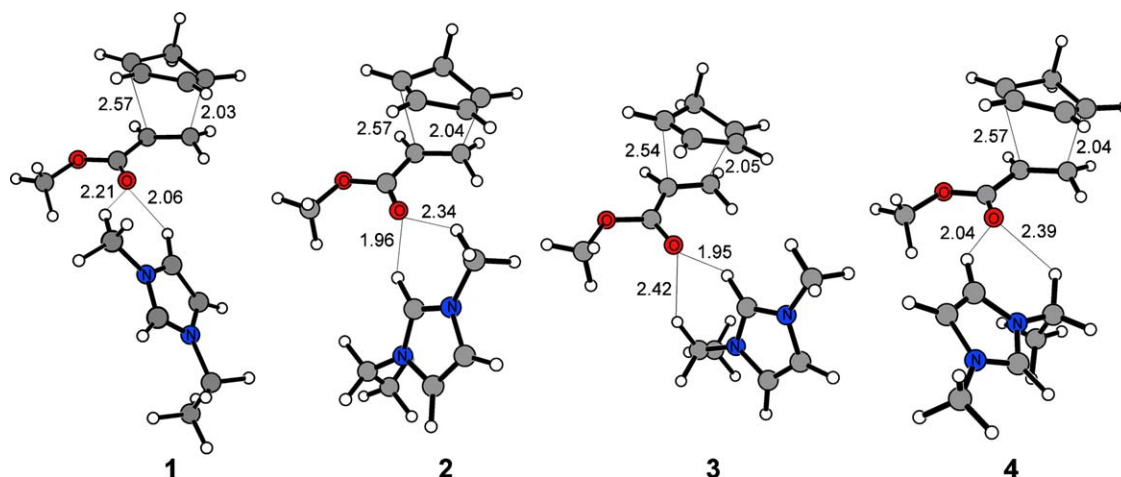


Fig. 3. *Endo-cis* transition structures with the 1-ethyl-3-methylimidazolium [EMIM] cation in configurations **1**–**4**, optimized using B3LYP/6-31G(d). Distances are in Å.

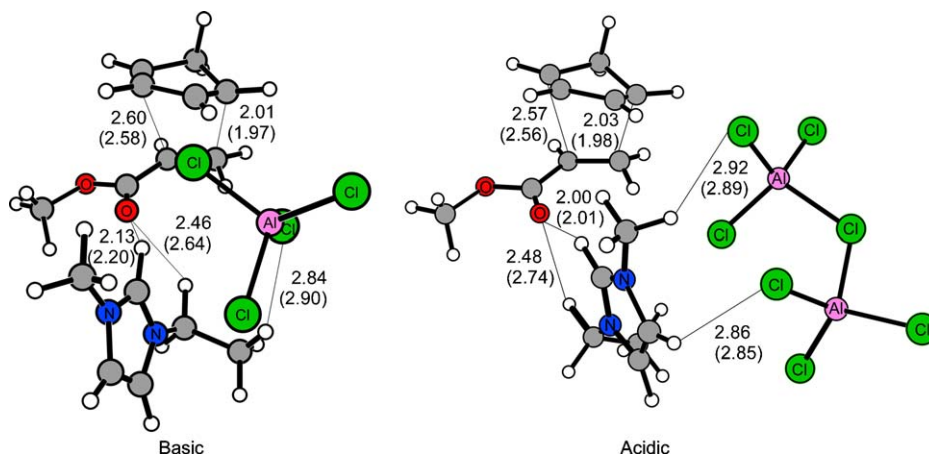


Fig. 4. The *endo-cis* transition structures complexed with 1:1 anion-to-cation chloroaluminate ionic liquids from B3LYP/6-31G(d) (B3LYP/6-311+G(2d,p) in parentheses) optimizations. Distances are in Å.

with the 6-31G(d) and 6-311+G(2d,p) basis sets (Tables 4 and 5). Multiple starting locations were attempted for the anion with the lowest-energy structures illustrated in Fig. 4. Increased stabilization of the transition structure in the “acidic” melt is reflected in the shorter ‘carbonyl oxygen–C2 hydrogen’ distance of 2.01 Å compared to 2.20 Å in the “basic” melt from the B3LYP/6-311+G(2d,p) geometries. The DFT calculations suggest that the [EMIM] cation functions as a Lewis acid modulated by the chloroaluminate anion, drawing more electron density from the dienophile when the ions are more loosely bound.

For a weak Lewis acid, such as water, subtracting the energies of an isolated cyclopentadiene and a methyl acrylate hydrogen bonded to 1–2 water molecules from the transition structure energy delivers a realistic picture of the energetic behavior [15]. However, from our prior ionic liquid study, using an isolated methyl acrylate complexed to an ionic liquid pair lead to activation energies that were superficially large [6]. In that case, the ionic environment did not partially quench the full ionic charges on the [EMIM] cation or the chloroaluminate anions. Alternatively, the activation barriers were computed in this study by subtracting the energies of the isolated cyclopentadiene, isolated methyl acrylate, and the isolated 1:1 ionic liquid complex from the total energy of the transition structure. Standard thermodynamic equations were used to convert the thermally corrected internal energy into enthalpies and Gibbs free energies at 25 °C via the ideal gas approximation [39].

The computed ΔG^\ddagger values for the “acidic” and “basic” melts using B3LYP/6-311+G(2d,p) were 37.6 and 37.5 kcal/mol, respectively (see Table 5). The predicted energies appear overestimated based on experimental ΔG^\ddagger values for a methanol/water mixture of 22.4 kcal/mol; [36] while the ionic liquids may not behave in a similar fashion to water, the activation barriers should be reasonably close (± 2 kcal/mol from transition state theory) based on reported rates for the Diels–Alder reaction in the aqueous-phase and in chloroaluminate ionic liquids [8]. In addition, the relative free energy difference between the “basic” and “acidic” melts using B3LYP/6-311+G(2d,p) is only 0.1 kcal/mol, which is significantly smaller than the experimental difference of 1.88 kcal/mol [8] or the 3.5 kcal/mol reported from QM/MM simulations [5]. It is likely that the entropy term, $T\Delta S$ at 298 K, is poorly represented in the DFT calculations. A previous computational study of aqueous-phase Diels–Alder reactions found that solvent effects were best captured by a discrete-continuum model, where half of the activation barrier lowering from gas to water came from local hydrogen-bonding (explicitly complexed water molecules) and half came from the bulk phase (modeled using the polarizable continuum model (PCM) [40])

[15]. In the present case, the ability of PCM to accurately represent the bulk-phase for a binary, purely ionic solvent is questionable.

The computed ΔH^\ddagger values of 13.8 and 14.5 kcal/mol for the “acidic” and “basic” melts at the B3LYP/6-311+G(2d,p) theory level appear more in-line with expectations as the ionic liquid lowered the enthalpic barrier by 7.0 and 6.3 kcal/mol compared to the gas-phase. In addition, the correct trend of the basic melt reporting a slower rate of reaction compared to the acidic melt was appropriately found. The favorable interactions between the acidic C2 proton and the carbonyl oxygen on methyl acrylate seem to indicate that DFT does a good quantitative job of representing the local effects for the reaction medium. However, the inability of DFT to predict the correct rates in terms of ΔG suggests that the entropy is highly dependent on an appropriate description of the bulk-phase. Currently, only a QM/MM simulation coupled to a Monte Carlo or molecular dynamics sampling method can realistically provide adequate computations on larger numbers of contributing ions by taking into account entropy, temperature, and enhanced sampling of the reactant with the solvent ions.

4.4. 2:1 “acidic” and “basic” melts

Increasing the number of anions further extends the electrostatic environment and potentially diminishes the Lewis acidity of the [EMIM] cation. The 2:1 complexes were approached in a similar fashion as for the 1:1 models with three unique transition structures involving two $[\text{AlCl}_4]$, a $[\text{AlCl}_4]$ and $[\text{Al}_2\text{Cl}_7]$, and two $[\text{Al}_2\text{Cl}_7]$ ions (Fig. 5 and Supporting Information Fig. S1). The distances between the most acidic [EMIM] hydrogen (on C2) and the carbonyl oxygen in the 2:1 basic melt complex were 2.19 Å, which compared favorably with the 2.20 Å distance for the 1:1 complex. However, in the case of the 2:1 acidic melt, the C2–carbonyl oxygen interacting distance of 2.14 Å was considerably longer than the 1:1 [EMIM][Al_2Cl_7] value of 2.01 Å. As expected, the two Al_2Cl_7 anions appear to better stabilize the positive charge on EMIM which reduces the cation’s ability to activate the transition structure to that of the basic melt, i.e. computed $\Delta H^\ddagger = 12.0$ and 11.5 kcal/mol for “acidic” and “basic” melts, respectively (Table 4).

The computed ΔG^\ddagger from the B3LYP/6-31G(d) calculations were 35.4–38.4 kcal/mol (see Table 5), placing the values reasonably close to that of the 1:1 models and the reported PDDG/PM3 results [5]. However, the predicted rate of reaction was opposite of experiment with the $\Delta\Delta G^\ddagger = 2.6$ kcal/mol greater for the 2:1 “acidic” over the 2:1 “basic” melt. The 2:1 anion-to-cation results should be taken strictly as qualitative indications of local

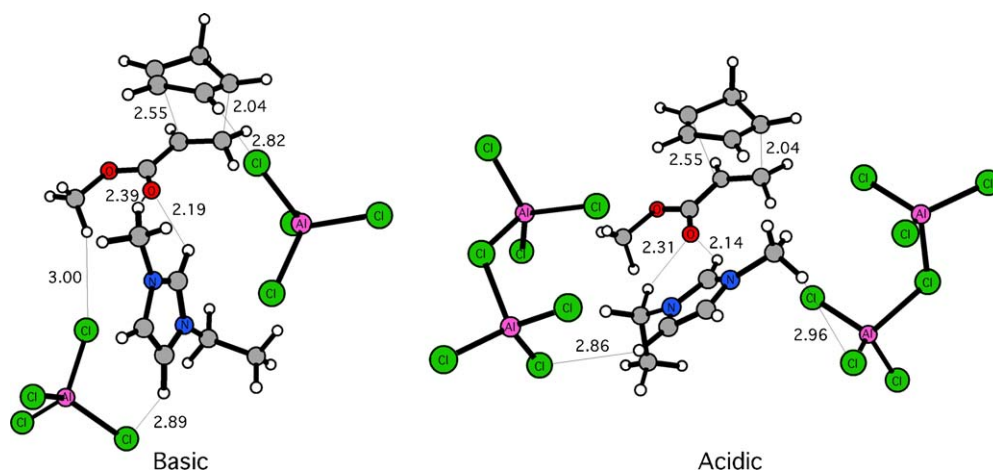


Fig. 5. The *endo-cis* transition structures complexed with 2:1 anion-to-cation chloroaluminate ionic liquids from B3LYP/6-31G(d) optimizations. Distances are in Å.

structuring of the ions around the Diels–Alder reaction owing to the fact that the overall charge is negative for this model (expected to be neutral in the liquid) which would undoubtedly affect the electronic structure and energy of the reaction.

5. Conclusions

The use of DFT in ascertaining the microscopic reasons behind the rate accelerations for the Diels–Alder reaction in ionic liquids proved to be erratic. Computations on the 1:1 anion-to-cation complexes reasonably predicted the activation enthalpy lowering for the “acidic” and “basic” melts relative to the gas-phase structure. However, the 1:1 complexes also incorrectly found a significantly smaller free energy difference between the melts, i.e. $\Delta\Delta G^\ddagger(\text{calc.}) = 0.1$ kcal/mol compared to 1.88 kcal/mol experimentally [8]. Thus, such truncated models that incorporate anticipated key interactions using high level quantum chemical computations do not appear to provide a realistic description of the bulk-phase environment in ionic liquids, likely owing to a poor description of the entropy term and the complexities of the electrostatics in the melts. The 2:1 anion-to-cation complexes gave more substantial deviations from experiment, incorrectly predicting the rate in the “basic” melt to be faster than in the “acidic”. However, the 2:1 model did qualitatively find the local structuring of the ions to be similar to that of the 1:1 complexes.

Recently reported QM/MM/MC simulations for the Diels–Alder reaction between cyclopentadiene and methyl acrylate in ionic liquids featured a semi-empirical model that yielded correct trends for relative rates of reactions, but overestimated activation barriers [5]. This has been also noted for other Diels–Alder reactions involving cyclopentadiene and three different dienophiles (acrylonitrile, methyl vinyl ketone, and 1,4-naphthoquinone) in different protic and aprotic solvents [38]. The present calculations suggest that the energetics computed for the Diels–Alder reaction via the DFT methodology provides reasonable results for the local interactions between the ions and the transition structure, however the explicit solvent ions do not adequately capture the bulk-phase solvent effects upon the reaction. The use of a DFT method in the computation of QM/MM/MC free energy profiles could improve the agreement with experiment, but the simulations would be computationally prohibitive from a practical standpoint as previous studies entailed ca. 20–80 million QM calculations.

In summary, the qualitative picture that emerges from the 1:1 transition structure complexes is that the reaction rate is greater in the “acidic” rather than the “basic” melt because ion-pairing is less

dominant in the “acidic” melt, thereby enabling the [EMIM] cations to better coordinate with the dienophile at the transition state. The coordination features hydrogen bonding with the more acidic ring hydrogens on [EMIM] and the dienophile’s carbonyl oxygen which is greater than that afforded by the weaker Lewis-acid effect with water molecules in aqueous solution [14,15,41].

Acknowledgements

Gratitude is expressed to the Alabama Supercomputer Center and Auburn University for support of this research. Discussions with Prof. Jeffrey D. Evanseck are highly appreciated.

Appendix A. Supplementary data

Supplementary data associated with this article can be found, in the online version, at [doi:10.1016/j.jmgs.2009.04.003](https://doi.org/10.1016/j.jmgs.2009.04.003).

References

- [1] (a) V.I. Pârvulescu, C. Hardacre, *Chem. Rev.* 107 (2007) 2615–2665; (b) F. van Rantwijk, R.A. Sheldon, *Chem. Rev.* 107 (2007) 2757–2785; (c) T. Welton, *Coord. Chem. Rev.* 248 (2004) 2459–2477.
- [2] X. Han, D.W. Armstrong, *Acc. Chem. Res.* 40 (2007) 1079–1086.
- [3] (a) M. Haumann, A. Riisager, *Chem. Rev.* 108 (2008) 1474–1497; (b) Z.C. Zhang, *Adv. Catal.* 49 (2006) 153–237.
- [4] (a) S.V. Sambasivarao, O. Acevedo, *J. Chem. Theory Comput.* 5 (2009) 1038–1050; (b) F. D’Anna, S. La Marca, R. Noto, *J. Org. Chem.* 73 (2008) 3397–3403; (c) F. D’Anna, V. Frenna, R. Noto, V. Pace, D. Spinelli, *J. Org. Chem.* 71 (2006) 5144–5150; (d) F. D’Anna, V. Frenna, V. Pace, R. Noto, *Tetrahedron* 62 (2006) 1690–1698.
- [5] O. Acevedo, W.L. Jorgensen, J.D. Evanseck, *J. Chem. Theory Comput.* 3 (2007) 132–138.
- [6] O. Acevedo, J.D. Evanseck, *Ionic Liquids as Green Solvents: Progress and Prospects*, ACS Symposium Series, vol. 856, 2003, 174–190.
- [7] A. Aggarwal, N.L. Lancaster, A.R. Sethi, T. Welton, *Green Chem.* 4 (2002) 517–520.
- [8] C.W. Lee, *Tetrahedron Lett.* 40 (1999) 2461–2464.
- [9] (a) T. Fischer, A. Sethi, T. Welton, Woolf, *J. Tetrahedron Lett.* 40 (1999) 793–796; (b) A. Kumar, S.S. Pawar, *J. Org. Chem.* 69 (2004) 1419–1420; (c) A. Kumar, S.S. Pawar, *J. Mol. Catal. A: Chem.* 208 (2004) 33–37.
- [10] R.V. Eldik, T. Asano, W. Le Noble, *Chem. Rev.* 89 (1989) 549–688.
- [11] J.A. Berson, Z. Hamlet, W.A. Mueller, *J. Am. Chem. Soc.* 84 (1962) 297–304.
- [12] S. Otto, W. Blokzijl, J.B.F.N. Engberts, *J. Org. Chem.* 59 (1994) 5372–5376.
- [13] M.P. Repasky, J. Chandrasekhar, W.L. Jorgensen, *J. Comput. Chem.* 23 (2002) 1601–1622.
- [14] J.F. Blake, D. Lim, W.L. Jorgensen, *J. Org. Chem.* 59 (1994) 803–805.
- [15] S. Kong, J.D. Evanseck, *J. Am. Chem. Soc.* 122 (2000) 10418–10427.
- [16] J. DeChancie, O. Acevedo, J.D. Evanseck, *J. Am. Chem. Soc.* 126 (2004) 6043–6047.
- [17] (a) A.D. Becke, *J. Chem. Phys.* 98 (1993) 5648–5652; (b) C. Lee, W. Yang, R.G. Parr, *Phys. Rev. B* 37 (1988) 785–789.
- [18] M.J. Frisch, *Gaussian 03, Revision A.1*, Gaussian Inc., Pittsburgh, PA, 2003 (full reference given in Supporting Information).

- [19] (a) M.C.C. Ribeiro, L.C.J. Almeida, *J. Chem. Phys.* 113 (2000) 4722–4731;
(b) G. Picard, F.C. Bouyer, M. Leroy, Y. Bertaud, S. Bouvet, *J. Mol. Struct. (Theochem)* 368 (1996) 67–80;
(c) P. Hébant, G. Picard, *J. Mol. Struct. (Theochem)* 358 (1995) 39–50;
(d) C.W. Bock, M. Trachtman, G.J. Mains, *J. Phys. Chem.* 98 (1994) 478–485.
- [20] O. Acevedo, J.D. Evanseck, *Org. Lett.* 5 (2003) 649–652.
- [21] C.L. Hussey, *Pure Appl. Chem.* 60 (1988) 1763–1772.
- [22] R.J. Gale, B.P. Gilbert, R.A. Osteryoung, *Inorg. Chem.* 17 (1978) 2728–2729.
- [23] J.S. Wilkes, J.S. Frye, G.F. Reynolds, *Inorg. Chem.* 22 (1983) 3870–3872.
- [24] (a) B.L. Ackermann, A. Tsarbopoulos, J. Allison, *Anal. Chem.* 57 (1985) 1766–1768;
(b) S.P. Wicelinski, R.J. Gale, K.M. Pamidimukkala, R.A. Laine, *Anal. Chem.* 60 (1988) 2228–2232.
- [25] J.L. Gray, G.E. Maciel, *J. Am. Chem. Soc.* 103 (1981) 7147–7151.
- [26] G. Franzen, B.P. Gilbert, G. Pelzer, E. Depauw, *Org. Mass Spectrom.* 21 (1986) 443–444.
- [27] C.J. Dymek Jr., D.A. Grossie, A.V. Fratini, W.W. Adams, *J. Mol. Struct.* 213 (1989) 25–34.
- [28] T.W. Couch, D.A. Lokken, J.D. Corbett, *Inorg. Chem.* 11 (1972) 357–362.
- [29] L.P. Davis, C.J. Dymek Jr., J.J.P. Stewart, H.P. Clark, W.J. Lauderdale, *J. Am. Chem. Soc.* 107 (1985) 5041–5046.
- [30] A.A. Fannin Jr., L.A. King, J.A. Leveisky, J.S. Wilkes, *J. Phys. Chem.* 88 (1984) 2609–2614.
- [31] A.A. Fannin Jr., D.A. Floreani, L.A. King, J.S. Landers, B.J. Piersma, D.J. Stech, R.L. Vaughn, J.S. Wilkes, J.L. Williams, *J. Phys. Chem.* 88 (1984) 2614–2621.
- [32] K.M. Dieter, C.J. Dymek Jr., N.E. Heimer, J.W. Rovang, J.S. Wilkes, *J. Am. Chem. Soc.* 110 (1988) 2722–2726.
- [33] A.K. Abdul-Sada, A.M. Greenway, K.R. Seddon, T. Welton, *Org. Mass Spectrom.* 24 (1989) 917–918.
- [34] S. Tait, R.A. Osteryoung, *Inorg. Chem.* 23 (1984) 4352–4360.
- [35] A.P. Scott, L. Radom, *J. Phys. Chem.* 100 (1996) 16502–16513.
- [36] M.F. Ruiz-López, X. Assfeld, J.I. García, J.A. Mayoral, L. Salvatella, *J. Am. Chem. Soc.* 115 (1993) 8780–8787.
- [37] (a) T.L. Amyes, S.T. Diver, J.P. Richard, F.M. Rivas, K. Toth, *J. Am. Chem. Soc.* 126 (2004) 4366–4374;
(b) J. Dupont, Spencer, *J. Angew. Chem. Int. Ed.* 43 (2004) 5296–5297.
- [38] O. Acevedo, W.L. Jorgensen, *J. Chem. Theory Comput.* 3 (2007) 1412–1419.
- [39] J.B. Foresman, A. Frisch, *Exploring Chemistry with Electronic Structure Methods*, second edition, Gaussian Inc., Pittsburgh, PA, 1996.
- [40] J. Tomasi, M. Persico, *Chem. Rev.* 94 (1994) 2027.
- [41] (a) J.F. Blake, W.L. Jorgensen, *J. Am. Chem. Soc.* 113 (1991) 7430–7432;
(b) J. Chandrasekhar, S. Shariffskul, W.L. Jorgensen, *J. Phys. Chem. B* 106 (2002) 8078–8085.
- [42] S. Takahashi, K. Suzuya, S. Kohara, N. Koura, L.A. Curtiss, M.L. Saboungi, *Z. Phys. Chem.* (1999) 209–222.